ANNALS of Clinical and Translational Neurology
Open Access
ANA American Neurological Association since 1875

RESEARCH ARTICLE

Dissociated multimodal hubs and seizures in temporal lobe epilepsy

Linda Douw[1,2,3], Matthew N. DeSalvo[1,2], Naoaki Tanaka[1,2], Andrew J. Cole[4], Hesheng Liu[1,2], Claus Reinsberger[1,5] & Steven M. Stufflebeam[1,2]

[1]Department of Radiology, Athinoula A. Martinos Center for Biomedical Imaging, Massachusetts General Hospital, Charlestown, Massachusetts
[2]Department of Radiology, Harvard Medical School, Boston, Massachusetts
[3]Department of Anatomy and Neurosciences, VU University Medical Center, Amsterdam, The Netherlands
[4]Department of Neurology, Massachusetts General Hospital, Boston, Massachusetts
[5]Department of Neurology, Brigham and Women's Hospital, Boston, Massachusetts

Correspondence
Linda Douw, Department of Anatomy and Neurosciences, Van der Boechorststraat 7, 1081 BT Amsterdam, The Netherlands. Tel: +31 20 444 5328; Fax: +31 20 444 8054; E-mail: douw@nmr.mgh.harvard.edu

Funding Information
This study was supported by NCRR (S10RR014978), National Institutes of Health (R01-NS069696, 5R01-NS060918, U01MH093765), and Dutch Organization for Scientific Research (NWO Rubicon 825.11.002).

Received: 3 December 2014; Revised: 22 December 2014; Accepted: 22 December 2014

Annals of Clinical and Translational Neurology **2015; 2(4): 338–352**

doi: 10.1002/acn3.173

Abstract

Objective: Brain connectivity at rest is altered in temporal lobe epilepsy (TLE), particularly in "hub" areas such as the posterior default mode network (DMN). Although both functional and anatomical connectivity are disturbed in TLE, the relationships between measures as well as to seizure frequency remain unclear. We aim to clarify these associations using connectivity measures specifically sensitive to hubs. **Methods**: Connectivity between 1000 cortical surface parcels was determined in 49 TLE patients and 23 controls with diffusion and resting-state functional magnetic resonance imaging. Two types of hub connectivity were investigated across multiple brain modules (the DMN, motor system, etcetera): (1) within-module connectivity (a measure of local importance that assesses a parcel's communication level within its own subnetwork) and (2) between-module connectivity (a measure that assesses connections across multiple modules). **Results**: In TLE patients, there was lower overall functional integrity of the DMN as well as an increase in posterior hub connections with other modules. Anatomical between-module connectivity was globally decreased. Higher DMN disintegration (DD) coincided with higher anatomical between-module connectivity, whereas both were associated with increased seizure frequency. DD related to seizure frequency through mediating effects of anatomical connectivity, but seizure frequency also correlated with anatomical connectivity through DD, indicating a complex interaction between multimodal networks and symptoms. **Interpretation**: We provide evidence for dissociated anatomical and functional hub connectivity in TLE. Moreover, shifts in functional hub connections from within to outside the DMN, an overall loss of integrative anatomical communication, and the interaction between the two increase seizure frequency.

Introduction

Temporal lobe epilepsy (TLE) has classically been seen as a disease limited to temporal structures. However, the rise of "connectomics" has changed this view. Connectomics are based on communication between brain areas, which may be measured with multiple imaging modalities. Resting-state functional magnetic resonance imaging (rsfMRI) allows for assessment of correlations between baseline oxygenation patterns, with particular brain areas showing similar fluctuations of activity at rest. One such subnetwork is the default mode network (DMN), consisting of the posterior cingulate cortex (PCC), precuneus, medial frontal cortex, parts of the temporal cortex, and inferior parietal areas.[1] DMN areas have high information throughput and are seen as major functional connectomic "hubs". If we equate functional connectomics to cars moving between cities, then the underlying highways are their anatomical counterparts. Anatomical connectomics can, among others, be measured by reconstructing white

matter pathways with diffusion MRI and counting the number of fibers connecting different brain areas.

TLE is characterized by altered functional and anatomical connectomics throughout the brain, leading to the current view of TLE as a network disease.[2,3] Functional disconnection occurs mainly within the DMN.[4–6] Anatomical connectivity is decreased globally,[7,8] but locally increases in DMN regions.[8,9] In healthy brains, anatomical and functional connectomics largely overlap, particularly in hub regions of the brain.[10,11] Diseases such as idiopathic epilepsy alter this usually tight-knit relationship.[12] In TLE, disturbed functional connectivity is related to altered white matter integrity, particularly in the posterior DMN.[5,13,14] However, the link between this apparent association and seizure vulnerability has not been investigated.

Moreover, simple correlations or number of fibers are likely not optimally sensitive to connectomic TLE pathology. Animal and computational studies suggest that seizure-like activity spreads most easily if the epileptogenic zone has high network importance, with a particularly important role for hubs serving long-distance communication.[15–19]

In this light, two interesting measures of hubness can be determined using "modularity." Modularity refers to the extent to which the brain can be divided into maximally intracorrelated subnetworks or modules based on its connectome.[20,21] This graph theoretical technique yields results similar to independent component analysis (ICA) in rsfMRI.[22] Generally, around four to ten brain modules are found, corresponding to known subsystems (e.g., DMN, motor system). Modular decomposition then allows for extensive investigation of connectivity within and across modules: within-module connectivity refers to an area's communication within its subnetwork, assessing local importance.[23] Between-module connections link multiple modules, transferring information over the entire network ("connector hubness"). Connector hubness in particular may be implicated in TLE, given that it relates to number of seizures and epilepsy-related protein expression in glioma patiens.[24]

We investigate the multimodal connectome in a large cohort of TLE patients. Although we investigate the entire brain, we expect that the DMN is the most affected functional module in TLE. Second, we hypothesize that particularly between-module connectomics relate to patients' seizure symptoms. Finally, dysfunctional anatomical connectomics are expected to mediate the association between altered functional connectomics and seizure symptoms.

Methods

Participants

Data were analyzed retrospectively after patient visits to Massachusetts General Hospital (MGH) between December 2009 and April 2013. All patients suffered from refractory TLE and were referred for presurgical imaging work-up. Inclusion criteria were age over 18 years and suspected TLE as determined by a specialized team of experienced epileptologists (N. T., A. J. C., C. R., S. M. S.) based on ictal video-EEG in accordance with the epilepsy classification by the International League Against Epilepsy (ILAE). Exclusion criteria were previous surgical intervention and neurological or psychiatric comorbidity. In addition to high-resolution imaging, clinical information was collected by medical chart review. Seizure frequency per month was extrapolated from patients' medical charts, and was only included when reported within 3 months of scanning date. Twenty-three healthy participants were also included, exclusion criteria being psychiatric or neurological disease and use of medication influencing the central nervous system. Hippocampal volumes were determined using FreeSurfer (http://surfer.nmr.mgh.harvard.edu) automatic segmentation procedures.[25]

Both the retrospective analysis of patient data and prospective inclusion of healthy controls was approved by MGH's institutional review board, and was performed in accordance with the Declaration of Helsinki. All healthy participants gave written informed consent before participation.

MRI data acquisition

The analysis pipeline is depicted in Figure 1. MRI data were collected using a 3T Siemens (Erlangen, Germany)

Figure 1. Schematic representation of analysis pipeline. Raw rsfMRI and DTI data underwent standard preprocessing and were coregistered to anatomical images (B), after which time series were extracted from the rsfMRI data (A) and projected onto the cortical surface. A 1000 parcel surface parcellation was used (D), and Pearson's correlation coefficients were calculated to obtain a connectivity matrix per subject (E), which contained 40% of the highest connections. Deterministic tractography was performed on voxelwise tensors calculated from the DTI images (C), and results were also projected to the surface parcellation. The number of connecting fibers per parcel (normalized for surface area size) was transformed into a connectivity matrix per subject. Weighted network analysis was performed on individual matrices per modality, yielding between a modularity index, and measures of within-module and between-module connectivity (G). Also, a group-averaged connectivity matrix (i.e., one for patients, one for controls) was calculated per modality, after which modularity analysis was run on these average matrices to obtain the benchmark modular structure per group and modality (F).

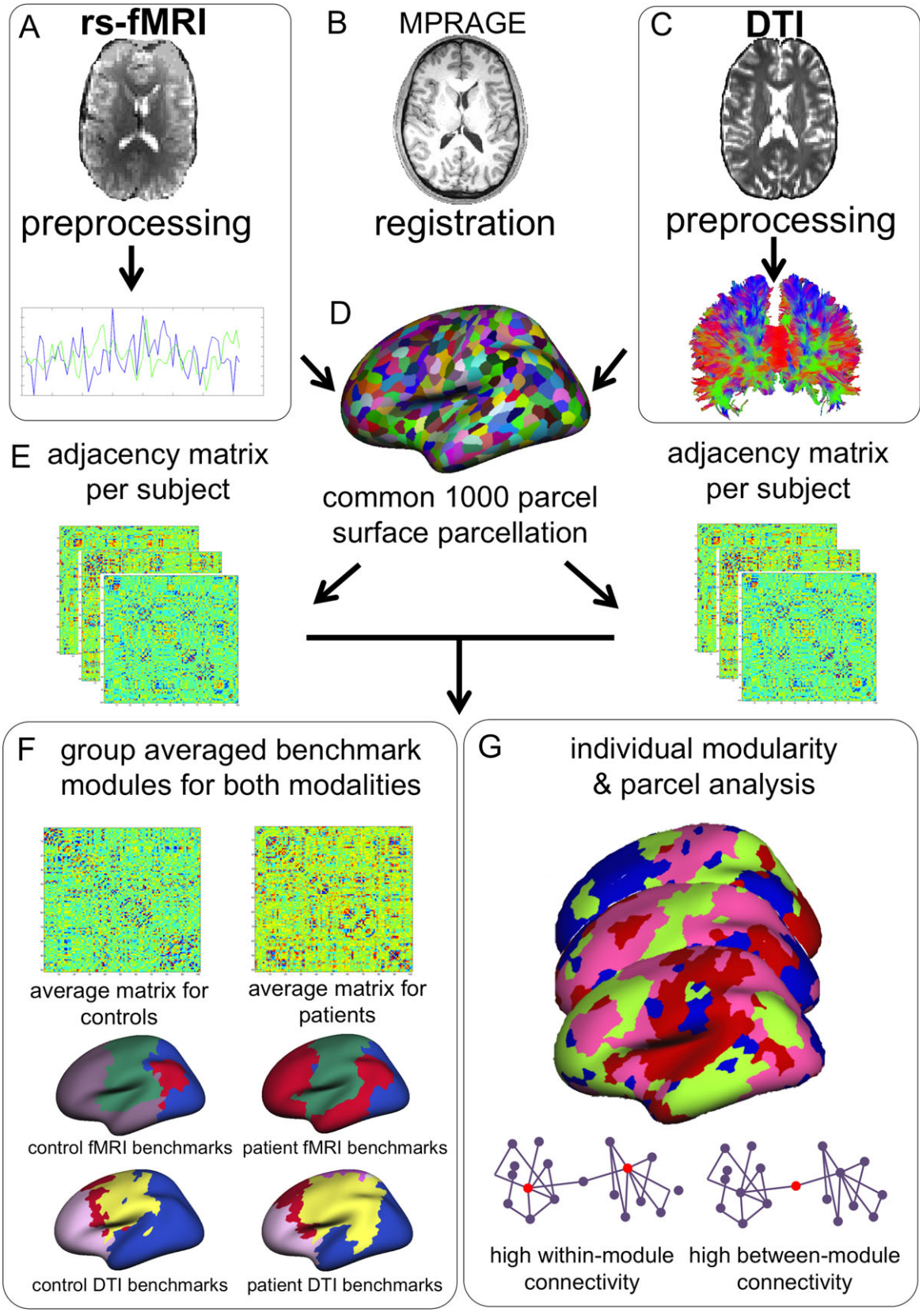

scanner with a 32-channel head coil. Anatomical images (multi-echo magnetization-prepared rapid acquisition with gradient echo [MEMPRAGE]), rsfMRI, and diffusion-weighted images (DTI) were collected. Scanning parameters of the MEMPRAGEs were as follows for patients: repetition time = 2530 msec, echo time = 1.74 msec, flip angle = 7°, field of view = 256, voxel size = 1 × 1 × 1 mm^3, 176 volumes; and for controls: repetition time = 2000 msec, echo time = 3.37 msec, flip angle = 10°, field of view = 256, voxel size = 1 × 1 × 1 mm^3, 160 volumes. In patients, rsfMRI was collected as follows: repetition time = 3000 msec, echo time = 30 msec, flip angle = 85°, field of view = 72, voxel size = 3 × 3 × 3 mm^3, 160 volumes, 8 min acquisition; and controls: repetition time = 5000 msec, echo time = 30 msec, flip angle = 90°, field of view = 128, voxel size = 2 × 2 × 2 mm^3, 76 volumes, 6.3 min acquisition, 2 runs. For DTI, scanning parameters for all participants were as follows: repetition time = 8080 msec, TE = 83 msec, flip angle = 90°, field of view = 128, voxel size = 1.85 × 1.85 × 1.85 mm, 10 b_0 volumes and 60 directional gradients at b = 700 sec/mm^2.

rsfMRI analysis

The Lausanne 2008 parcellation scheme was used for analysis of 1000 cortical surface parcels.[26,27] This parcellation is based on the Desikan atlas,[28] after which the cortical surface is further divided into areas with approximately the same size (1.5 mm^2).

During rsfMRI, participants fixated their gaze and were instructed to stay awake without thinking about anything in particular. Participants with more than 3 mm absolute head movement during rsfMRI were excluded. Standard preprocessing of rsfMRI data included (1) discarding the first four volumes of each run to ascertain T1-equilibrium, (2) slice timing correction, (3) head motion correction with FSL,[29] (4) removal of constant offset and linear trend per run, (5) low-pass filtering below 0.08 Hz, (6) regressing out of six motion parameters, average signal of the whole brain, ventricles, and white matter.[30] Participants' individual functional images were projected onto a template cortical surface, after which a 6 mm full-width half-maximum (FWHM) smoothing kernel was applied to the surface data, and data were down sampled to 4 mm resolution. Average time series were then extracted from each parcel, and Pearson's correlation coefficients between each pair yielded a 1000 × 1000 fMRI connectivity matrix per subject. In order to eliminate negative correlations but avoid disconnection of some parcels, a proportional threshold retaining the top 40% of all connections was applied to each connectivity matrix (see Results for detailed information on this choice of threshold).

Diffusion analysis

Diffusion data were visually inspected for motion, including only data without visible motion. Connectome Mapper software was used to analyze DTI data.[27] Anatomical volumes were registered to B_0 volumes using a rigid body alignment with FLIRT from the FSL toolbox (http://fsl.fmrib.ox.ac.uk/fsl/fslwiki/). Diffusion tensors per voxel were reconstructed using the Diffusion Toolbox (www.trackvis.org/dtk), after which deterministic streamline tractography (angle threshold = 60°) was performed on the entire white matter using 32 random seed points per voxel.[31] Fibers were filtered for length (2–50 cm) and spline filtered for smoothing. Then, an adjacency matrix was generated for each subject by weighing the number of determined connecting fibers by the size of each ROI's surface area.[26] We also corrected for linear bias toward longer fibers introduced by tractography, as this correction has been shown to lead to reduced intra-subject variability between scans.[32]

Within-module and between-module connectivity

The Brain Connectivity Toolbox[33] and custom-made scripts (Matlab r2012a; Mathworks (Natick, MA, USA) were used for network analysis. These analyses were performed identically on rsfMRI and DTI connectivity matrices. Newman's modularity algorithm was used to calculate the optimal modular division into strongly intraconnected but weakly interconnected modules for each participant, in which each parcel received a single module allegiance,[20] as follows:

$$Q^{\mathrm{w}} = \frac{1}{l^{w}} \sum_{ij \epsilon N} \left[\mathrm{w}_{ij} - \frac{k_i^{\mathrm{w}} k_j^{\mathrm{w}}}{l} \right] \delta_{m_i, m_j}$$

in which l^{w} is the weight of all links in the network, w_{ij} is the connection weight between nodes i and j (within the total set of network nodes N), k_i^{w} is the weighted degree of node i, and δ_{m_i,m_j} refers to differences in community index between nodes i and j.

Subsequently, connectivity of each parcel within its own module and between several modules was calculated.[23,33] Within-module connectivity assesses a parcel's connectivity within its own module; high values indicate importance on the local (in terms of network neighbors, not spatial closeness), segregated level:

$$z_i^{\mathrm{w}} = \frac{k_i^{\mathrm{w}}(m_i) - \overline{k^{\mathrm{w}}}(m_i)}{\sigma^{k^{\mathrm{w}}(m_i)}}$$

where m_i is the module containing node i, $k_i^{\mathrm{w}} m_i$ is the weight of all links between i and all other nodes in m_i, and $\overline{k^{\mathrm{w}}}(m_i)$ and $\sigma^{k^{\mathrm{w}}(m_i)}$ are the respective mean and standard deviation of the within-module weight distribution.

Conversely, weighted between-module connectivity calculates how strongly a node is connected to other nodes outside its own module:

$$y_i^{\mathrm{w}} = 1 - \sum_{m \epsilon M} \left(\frac{k_i^{\mathrm{w}}(m)}{k_i^{\mathrm{w}}} \right)^2$$

in which y_i^{w} refers to the weighted participation coefficient of node i, M is the set of modules m calculated with the modularity algorithm described above, $k_i^{\mathrm{w}}(m)$ is the weight of links between i and all nodes in m, and k_i^{w} is the weight of all links in the network. Nodes with high between-module connectivity link different subsystems of the brain across longer distances and can be termed connector hubs.

Because the solution to the modular subdivision may differ on each run of the algorithm,[34] modularity analysis was run 1000 times, after which values of between and within-module connectivity were averaged.

Functional DD

Functional disconnection of the DMN was expected in TLE, with losses of connectivity between its anterior and posterior parts. Therefore, modular connectivity within this functional module was quantified by a DMN disintegration (DD) score, defined here as intramodular connectivity in the anterior part divided by intramodular connectivity in the posterior part of the DMN. DD values around 1 indicate preserved modular DMN dynamics, while deviating values indicate a shift in DMN modular connectivity toward less integrated functioning and more outward connectivity in either of the two DMN components.

Statistical analysis

Statistical analysis was performed with PASW Statistics IBM Corp (Armonk, NY, USA) (version 20) and Matlab. Group differences in subject characteristics were tested using Student's *t*-tests for independent samples and chi-square tests. Group differences in modular connectivity were tested with regression analyses, and were corrected for multiple testing using the false discovery rate (FDR).[35] Covariates entered into all group-level analyses were age, sex, hippocampal volumes, and relative motion.

Within patients, associations between anatomical and functional modular connectomics were tested with regression analyses, as were correlations of multimodal modular connectivity and seizure frequency/duration. Age, sex, hippocampal volumes, motion, lateralization of TLE, and presence/absence of visible lesions on MRI were always included as covariates in these within-patient analyses.

Finally, mediation effects were tested using the INDIRECT PASW statistics plug-in.[36] The presence of mediation signifies that instead of having a direct effect between the independent variable (functional hub connectivity) and dependent variable (seizure frequency/duration); the mediator (anatomical hub connectivity) plays an important role in the association between these two variables. Mediation involved regression analyses to test these direct and indirect effects, after which 95% CIs were calculated for the total indirect effects using bootstrapping (10,000 samples) as an unbiased means of model validity testing. Based on above-mentioned analyses, only significant covariates (age, sex, motion) were taken into account.

Level of statistical significance was set at group-wise $P < 0.05$ for all analyses, taking multiple comparisons into account.

Results

Subject characteristics

Forty-nine TLE patients and 23 controls participated (Table 1), after exclusion of two eligible patients showing excessive motion during scanning. Thirty-two patients had left-sided TLE (LTLE), whereas 17 had right-lateralized epilepsy (RTLE). LTLE patients had significantly higher seizure frequency (16.0 ± 24.6) than RTLE patients (4.7 ± 7.6; $t(40) = 2.181$, $P = 0.037$), but these groups did not differ regarding other clinical parameters. Nineteen patients did not show lesions on 3T MRI. Most patients with lesions on MRI had suspected mesial temporal sclerosis (MTS) or cortical dysplasia, with one patient showing a cavernous malformation and one patient having an area of heterotopia. Although none of the patients had undergone surgery before rsfMRI and DTI, information regarding outcome of surgery performed after scanning mostly supports suspected diagnoses. Surgery was performed in 18 of the total 49 patients with a follow-up of 1 year at the time of writing (20 in total), with most (i.e., 14 or 78%) patients being seizure-free at least 1 year after resection of the affected temporal lobe (Engel class I[37]). Two patients had meaningful reductions in seizure frequency 1 year post

Table 1. Patient characteristics.

	Patients (n = 49)	Controls (n = 23)
Age in years, M (SD)	36.9 (13.0)	21.8 (3.1)*
Males (females)	23 (26)	7 (16)
Age of onset, M (SD)	21.1 (13.7)	
Seizure duration in years, M (SD)	15.4 (13.6)	
Monthly seizure frequency, M (SD), n = 40	11.7 (20.5)	
Handedness: right/left/ambidexter/unknown	35/7/4/3	23/0/0/0
Left hippocampal volume, mm^3 M (SD)	3932.9 (721.9)	4416.6 (386.3)
Right hippocampal volume, mm^3 M (SD)	4104.3 (540.6)	4393.4 (373.5)
MRI findings: no lesion/MTS/cortical dysplasia/other	19/24/3/3	
Pathology: no lesion/MTS/other, n = 25	4/20/1	
Postsurgical outcome Engel class I/II–III/IV, n = 25	19/3/3	
No of AEDs used (1/2/3/4/unknown)	6/25/10/5/3	

MRI, magnetic resonance imaging; MTS, mesial temporal sclerosis; AEDs, Anti-epileptic drugs.
*$P < 0.01$ difference between patients and controls.

surgery (Engel class II–III), whereas two patients did not benefit from the intervention (Engel class IV).

Information on monthly seizure frequency and duration within 3 months of scanning was reliably noted in the medical chart of 42 patients. Higher seizure frequency was related to longer disease duration (Pearson's rho = 0.327, 95% CI with 1000 bootstrapping samples 0.086 to 0.639, $P = 0.034$). Patients were older (95% CI 9.556 to 20.587 years, $P < 0.001$, see Table 1) and had more relative head motion (95% CI 0.007 to 0.137 mm, $P = 0.030$) than controls.

Functional and anatomical spatial modular decomposition

Group-level modular topology was spatially investigated by obtaining a "benchmark" healthy modular subdivision, that is, averaging all controls' matrices and performing modularity analysis on this averaged matrix as described previously.[38] The same analysis was performed in patients. There were three modules in the healthy benchmark network (Fig. 2A). One module spanned areas of the classical DMN, as well as association and frontal cortex, which will be referred to as the DMN+. Another module included the precentral and postcentral gyri, and some superior temporal cortex, which we termed the sensorimotor module (SMM). Finally, a module encompassing visual and parietal areas was termed the parieto-occipital module (POM). In patients, benchmark analysis yielded four modules (Fig. 2B), with the DMN+ disconnected into separate anterior and posterior parts (aDMN+ and pDMN+, respectively), as expected and further illustrated in Figure 3. When looking at participants' individual modular decomposition, all but one control had intact DMN+ (96%), whereas 27 patients (55%) showed disconnection (chi-square $P < 0.001$). Of the total 49 patients, 44 had three (20% or 45%) or four (24% or 55%) modules. Three patients had two modules, whereas two patients had five modules. Patients' individual modules particularly overlapped less spatially with the pDMN+, as determined by Dice indices (Table 2).[39]

Anatomically, nine modules were found in the healthy benchmark modular connectome, whereas patients' averaged connectivity matrix yielded seven modules (Fig. 2C and D). There were no significant group differences in individual spatial overlap with the benchmark modules (Table 2).

Functional hub connectivity

All following analyses took place on participants' individual modular decomposition and subsequent calculation of hub connectivity. In TLE patients, the DMN+ was characterized by lower within-module connectivity overall, although not significantly after FDR correction (Table 3). Furthermore, the DMN+ showed a shift in between-module hub connectivity from its anterior to its medial posterior parts (Fig. 4). The POM displayed fewer connections to other modules in TLE, but higher within-module connectivity.

Within patients, DD trended toward correlation with seizure frequency when correcting for all covariates (regression B 95% CI −3.769 to 45.596, $P = 0.094$), although none of the covariates (age, sex, TLE lateralization, hippocampal volumes, visible lesion on MRI, motion) were significant. When removing all covariates except age and gender, the beta coefficients were similar but statistical significance improved greatly (regression B 95% CI 3.391 to 46.630, $P = 0.025$), suggesting that statistical power was limited when using a number of noninfluential predictors. No associations were present with seizure duration (Table 4), and addition of seizure duration barely changed statistical significance of the association between DD and seizure frequency (regression B 95% CI −1.533 to 42.399, $P = 0.067$). POM hub connectivity was not associated with seizure frequency or duration.

Anatomical hub connectivity

Patients showed widespread losses of between-module connectivity (Fig. 4). This loss was found in the DMN+ (functionally defined as the patient benchmark aDMN+ and pDMN+), as well as when globally averaging over all

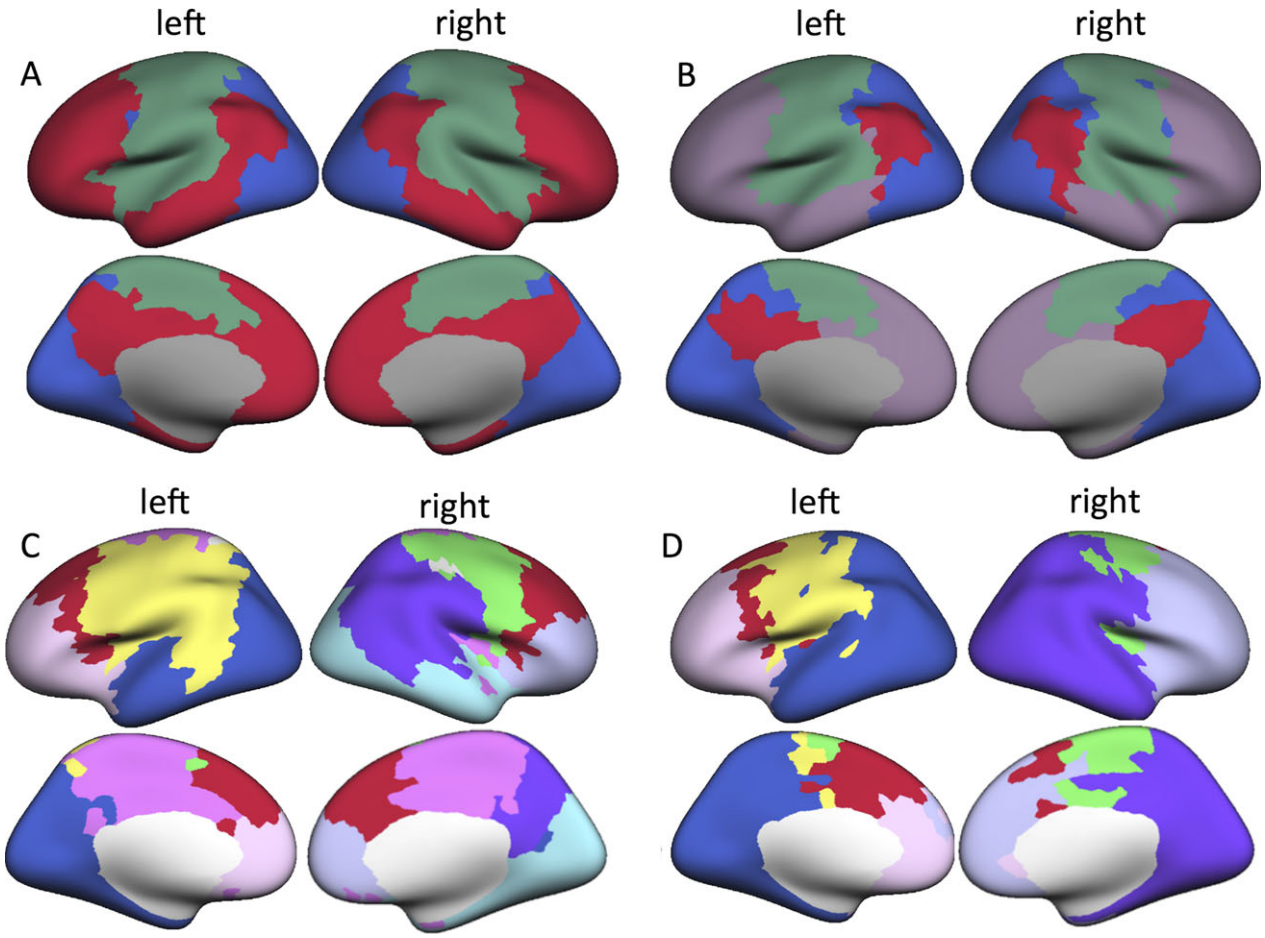

Figure 2. Modular topology in patients and controls. (A) Functional benchmark modules in healthy controls. Crimson red indicates the default mode network (DMN+), green indicates the sensorimotor module (SMM), and blue refers to the parieto-occipital module (POM). In temporal lobe epilepsy (TLE) patients (B), violet refers to the anterior default mode network (aDMN+) and crimson red to the posterior default mode network (pDMN+). (C) Displays anatomical benchmark modules in healthy controls, whereas (D) depicts average modular structure in TLE patients.

parcels (Table 3), indicating a general phenomenon. Within-module connectivity was not statistically different between groups after FDR correction, whereas it was lower in the averaged pDMN+ in TLE patients. RTLE patients had lower between-module connectivity (0.087 ± 0.04) than LTLE patients (0.162 ± 0.07; regression B 95% CI 1.658 to 5.236, $P < 0.001$). However, both LTLE and RTLE groups' values were lower than controls (0.220 ± 0.03; regression B 95% CI −7.732 to 0.143, $P = 0.042$, and regression B 95% CI −7.274 to 4.329, $P < 0.001$, respectively).

Within patients, global between-module connectivity was positively correlated with monthly seizure frequency (Table 4). There were no significant effects of age, sex, TLE lateralization, hippocampal volumes, visible lesion on MRI, or motion. It was not associated with seizure duration, and adding duration to the regression model involving seizure frequency did not change results.

Functional and anatomical hub connectivity and seizures

In patients, functional DD and anatomical between-module connectivity were positively correlated (regression B coefficient 95% CI 0.171 to 2.482, $P = 0.025$, Fig. 5): indicating that lower, more disturbed anatomical between-module connectivity correlated with less dysfunctional DMN+. There were no significant effects of age, sex, TLE lateralization, hippocampal volumes, visible lesion on MRI, or motion. This association was present in LTLE and RTLE groups separately (TLE lateralization regression B coefficient 95% CI −0.086 to 0.226, $P = 0.373$).

We then tested whether global anatomical between-module connectivity mediated the association between functional DD and seizure frequency. The association between DD and higher seizure frequency proved to be mediated by higher anatomical between-module connec-

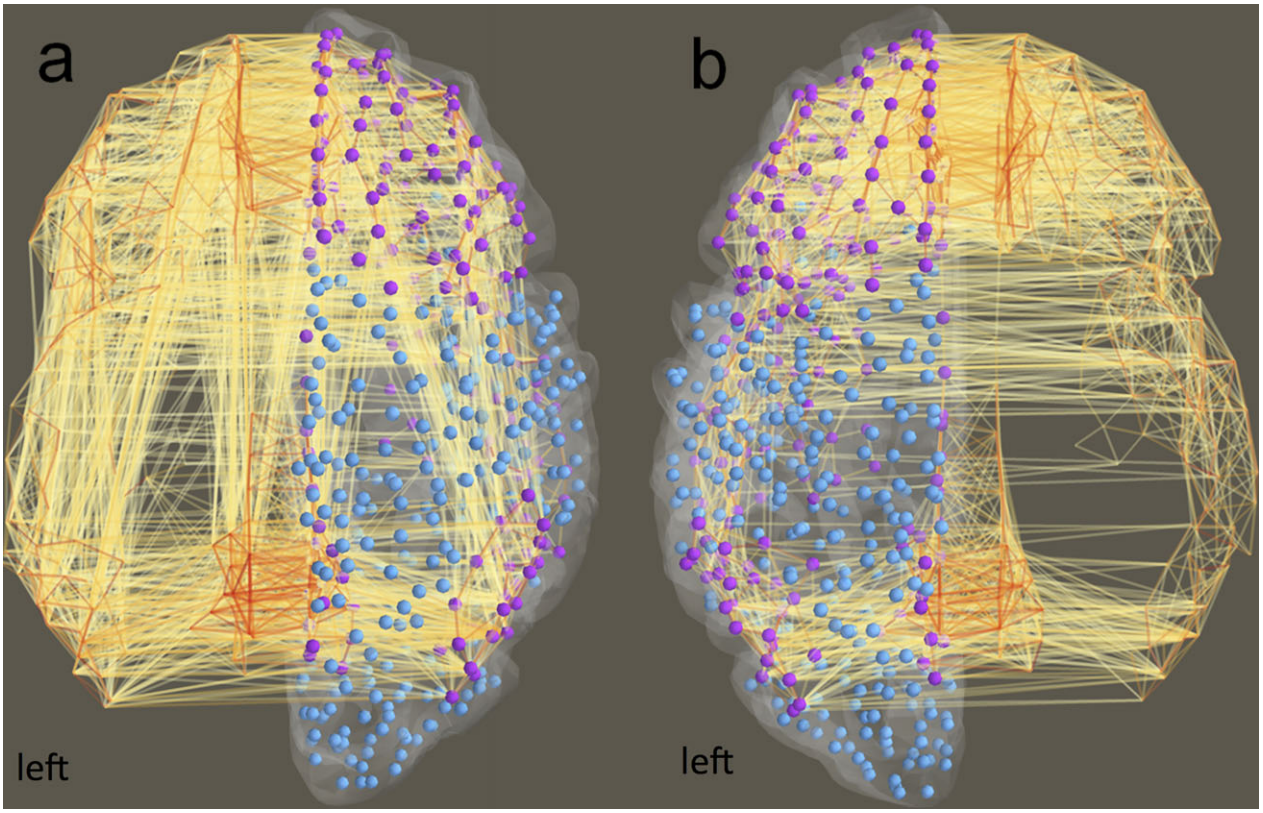

Figure 3. Within-module DMN+ connections in patients versus controls. Purple nodes indicate the aDMN+ and pDMN+, blue nodes are the parcels outside of the DMN+. (A) Depicts all within-module connections in healthy controls, (B) displays those within-module connections in TLE patients. aDMN+/pDMN+, anterior/posterior default mode newtork; TLE, temporal lobe epilepsy.

Table 2. Dice indices between individual and benchmark modules in patients and controls.

	Dice index		Group difference		
Benchmark module	M controls (SD)	M patients (SD)	B [95% CI]	*t*	*P*-value
Functional network					
aDMN+	0.613 (0.0703)	0.607 (0.114)	−0.203 [−1.200 to 0.709]	−0.407	0.685
pDMN+	0.450 (0.143)	0.252 (0.0613)	2.023 [1.393 to 2.653]	6.413	<0.001*
SMM	0.642 (0.116)	0.569 (0.135)	0.250 [−0.566 to 1.066]	0.612	0.543
POM	0.595 (0.117)	0.660 (0.117)	−0.859 [−1.58 to −0.138]	−2.379	0.020
Anatomical network					
Right lateral motor	0.273 (0.175)	0.182 (0.146)	0.781 [0.196 to 1.366]	2.665	0.010
Medial motor	0.288 (0.169)	0.215 (0.136)	0.445 [−0.192 to 1.081]	1.395	0.168
Left lateral motor	0.295 (0.136)	0.241 (0.169)	0.125 [−0.506 to 0.757]	0.396	0.694
SMA	0.285 (0.189)	0.223 (0.117)	0.441 [−0.214 to 1.096]	1.344	0.183
Left occipital	0.293 (0.212)	0.242 (0.173)	0.231 [−0.282 to 0.744]	0.900	0.371
Right parietal	0.347 (0.233)	0.218 (0.145)	0.664 [0.167 to 1.162]	2.668	0.010
Right occipital	0.327 (0.278)	0.253 (0.183)	0.377 [−0.055 to 0.810]	1.743	0.086
Right frontal	0.201 (0.184)	0.221 (0.149)	−0.002 [−0.610 to 0.606]	0.007	0.995
Left frontal	0.312 (0.231)	0.189 (0.144)	0.621 [0.117 to 1.125]	2.460	0.017

All regression models corrected for motion, age, sex, and hippocampal volumes. aDMN+/pDMN+, anterior/posterior default mode network; SMM, sensorimotor network module; POM, parieto-occipital module; SMA, supplementary motor area.
*$P < 0.05$ (after FDR correction).

Table 3. Group differences in modular connectivity

	M patients (SD)	M controls (SD)	B [95% CI]	*t*	*P*-value
Functional connectome					
Between-module					
aDMN+	0.440 (0.115)	0.492 (0.005)	0.728 [−0.274 to 1.729]	1451	0.152
pDMN+	0.470 (0.116)	0.451 (0.014)	−0.768 [−1.797 to 0.262]	−1490	0.141
SMM	0.484 (0.116)	0.457 (0.006)	−0.497 [−1.550 to 0.555]	−0.944	0.349
POM	0.432 (0.118)	0.475 (0.005)	0.601 [−0.407 to 1.610]	1190	0.238
Within-module					
aDMN+	−0.066 (0.178)	−0.0001 (0.031)	0.803 [0.163 to 1.443]	2507	0.015
pDMN+	−0.132 (0.379)	0.003 (0.057)	0.363 [0.055 to 0.670]	2355	0.022
SMM	−0.013 (0.237)	−0.003 (0.043)	−0.241 [−0.748 to 0.267]	−0.948	0.347
POM	0.139 (0.150)	0.003 (0.034)	−1.290 [−1.926 to −0.653]	−4048	<0.001*
Anatomical connectome					
Between-module					
Global average	0.134 (0.070)	0.219 (0.030)	2.673 [1.358 to 3.988]	4060	<0.001*
Functional aDMN+	0.127 (0.066)	0.205 (0.042)	2.470 [1.053 to 3.886]	3481	0.001*
Functional pDMN+	0.136 (0.083)	0.254 (0.047)	2.452 [1.483 to 3.421]	5053	<0.001*
Within-module					
Functional aDMN+	0.005 (0.055)	0.018 (0.063)	0.743 [−0.942 to 2.427]	0.880	0.382
Functional pDMN+	0.136 (0.083)	0.254 (0.047)	0.901 [0.316 to 1.486]	3077	0.003*

All regression models corrected for motion, age, sex, and hippocampal volumes. aDMN+/pDMN+, anterior/posterior default mode network; SMM, sensorimotor network module; POM, parieto-occipital module.
*$P < 0.05$ (after FDR correction).

tivity (Fig. 6; 95% CI 2.723 to 25.092). Additionally, a mediation model with higher seizure frequency relating to increasing anatomical modular connectivity through higher DD also yielded significant results (Fig. 6; 95% CI 0.0001 to 0.0011).

Role of possible confounders

Age

We controlled for the group age difference by adding this confounder to all analyses. In order to completely rule out that the difference in age between patients and controls caused our findings, we also repeated group analyses on a subsample consisting of controls and the 23 youngest patients (mean 25.9 ± 5.14 years). This analysis yielded predominantly identical results, apart from an increased *P*-value of the association between functional DD and seizure frequency (beta coefficient 95% CI −0.379 to 129.08, $P = 0.051$), possibly due to reduced statistical power in this smaller sample. More importantly, the investigation of the association between anatomical and functional modular connectivity within patients is separate from controls and thus not influenced by this group difference in age.

Subject motion

Since group differences in motion may influence connectivity and network findings[40,41] and patients showed higher motion than controls in our study, we also repeated all analyses using a subsample of patients with motion equal to controls (patients $n = 32$, both groups relative motion mean 0.08 mm, range [0–0.15] mm, two-tailed Student's *t*-test 95% CI −0.020 to 0.017, $P = 0.862$). Results were identical, apart from the association between DD and seizure frequency, which lost significance but remained a statistical trend when taking age and sex into account (regression B 95% CI −1.953 to 65.74, $P = 0.064$).

AED use

The influence of anti-epileptic drugs (AEDs) on connectivity and networks is largely unknown. Furthermore, most patients in our study used multiple AEDs with highly variable AED combinations, rendering controlling for this factor difficult. We did test whether the number of different AEDs used (monotherapy vs. polytherapy as well as number of AEDs from 1 to 4) influenced our results. This proved not to be the case, and neither variable was ever significant as a covariate.

Functional connectivity threshold

Another common confounder in functional network analysis is the choice of functional connectivity threshold in rsfMRI, as negative correlations are incompletely understood physiologically. We retained the 40% highest connections, because this proportional threshold signified the highest number of connections (and thus information) we were able to retain without also including nega-

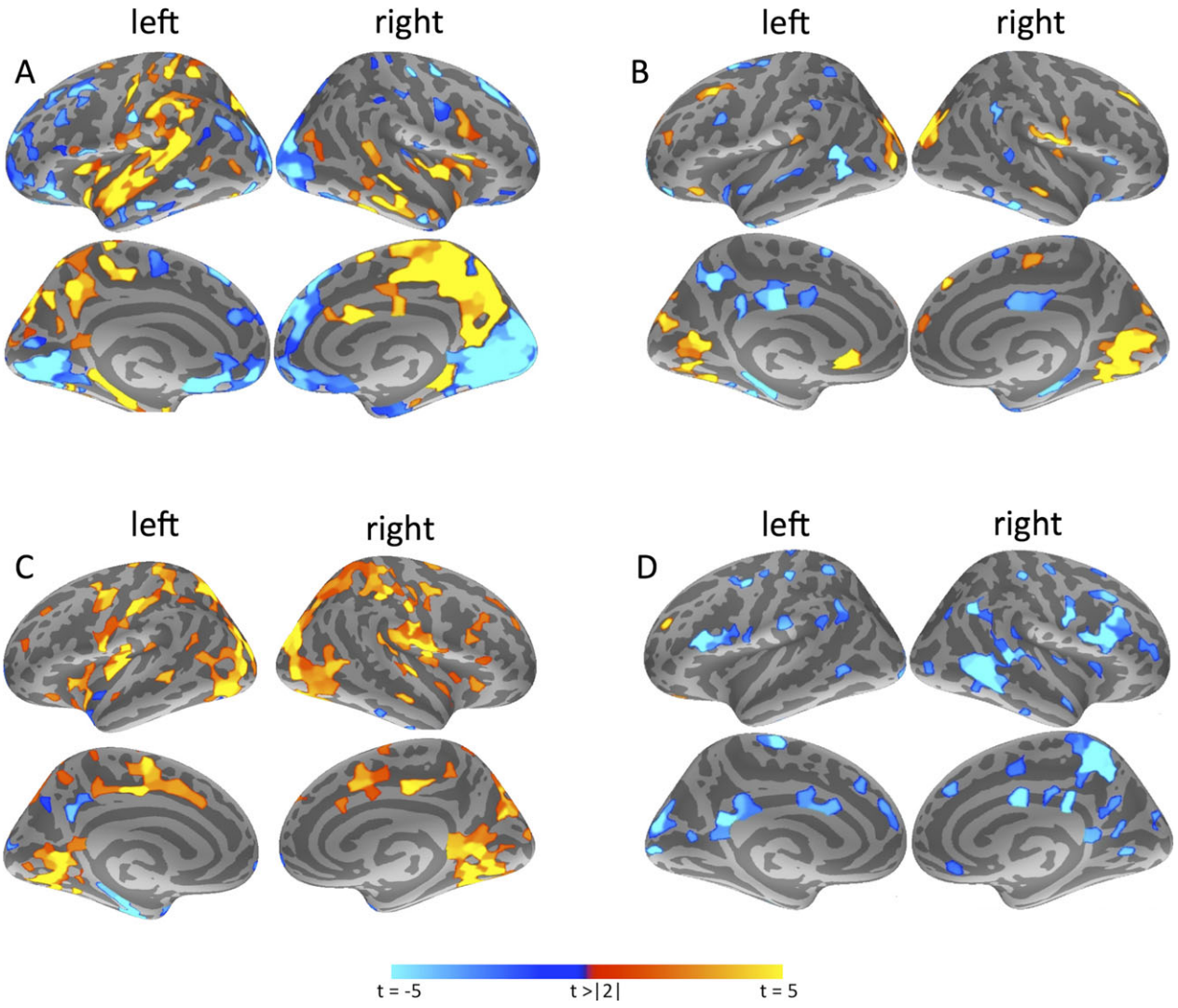

Figure 4. Group differences in modular connectivity. All displayed results are significant with $P < 0.05$ after false discovery rate (FDR)-correction for multiple testing and correction for covariates. (A) Displays differences in functional between-module connectivity in patients as compared to controls. Warm colors indicate higher connectivity in patients, cool colors signify higher connectivity in controls. (B) Indicates functional within-module connectivity in patients versus controls, whereas (C) shows differences in regular functional connectivity per parcel. In (D), anatomical between-module differences are depicted. There were no significant parcel-based differences between groups in within-module or regular anatomical connectivity after correcting for confounders and multiple testing.

tive correlations. Furthermore, using a proportional threshold prevents a priori interindividual differences causing connectivity network topology differences. In order to investigate the robustness of our results with respect to choice of threshold, we repeated our analyses using 20% and 30% of the connections, but these analyses did not yield different results.

Functional modularity methods

Functional modularity analysis usually results in a resting-state network structure comparable to other methods of dividing the brain into meaningful subsystems.[22] In order to compare to other commonly used methods of resting-state analysis, we replicated our data-driven results with a seed-based approach. The averaged control connectivity matrix was used to seed each resting-state network, and all connections with Pearson's rho >0.3 were included per module.[42] These analyses yielded smaller networks and more significant results in general, but findings in terms of differences in module overlap between patients and controls did not change.

Table 4. Associations between modular connectivity and patients' clinical status.

	Seizure frequency			Seizure duration		
	B [95% CI]	*t*	*P*-value	B [95% CI]	*t*	*P*-value
Functional connectome						
DD	20.91 [−3.769 to 45.60]	1.724	0.094	7.979 [−4.150 to 20.11]	1.331	0.191
POM within-module	26.54 [−20.75 to 73.82]	1.142	0.262	1.039 [−22.11 to 24.19]	0.091	0.928
Anatomical connectome						
Between-module						
Global	155.8 [40.73 to 270.9]	2.752	0.009*	−20.08 [−83.04 to 42.87]	−0.645	0.523
Functional aDMN+	122.3 [−6.620 to 251.2]	1.928	0.062	−11.80 [−79.03 to 55.50]	−0.453	0.725
Functional pDMN+	118.4 [23.09 to 213.6]	2.525	0.016*	−26.82 [−78.59 to 24.95]	−1.047	0.301

All regression models corrected for motion, age, sex, and hippocampal volumes. aDMN+/pDMN+, anterior/posterior default mode network; POM, parieto-occipital module; DD, modular DMN+ (extended default mode network) disintegration.
*$P < 0.05$ (after FDR correction).

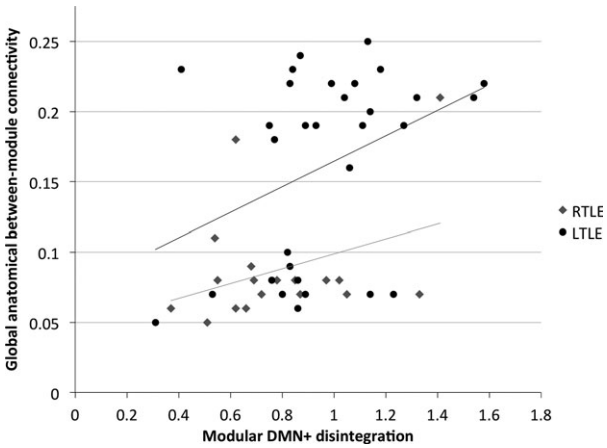

Figure 5. Correlation between modular default mode network (DMN+) disintegration and anatomical between-module connectivity. TLE lateralization is depicted separately, with right temporal lobe epilepsy (RTLE) patients showing lower anatomical between-module connectivity than left temporal lobe epilepsy (LTLE) patients. The association between functional modular DMN+ disintegration and anatomical between-module connectivity is present in the sample as a whole, and the two groups separately.

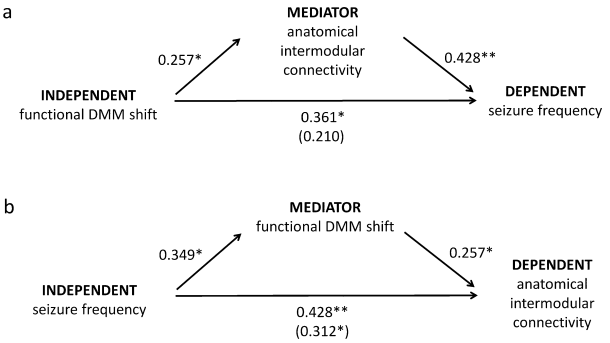

Figure 6. Mediation analyses of the associations between functional default mode network (DMN+) shift, anatomical between-module connectivity loss, and monthly seizure frequency. *$P < 0.05$, **$P < 0.01$. Numbers next to arrows are normalized coefficients in regression models, with the normalized coefficients when taking the mediator into account in parentheses.

Discussion

TLE patients have disturbed functional and anatomical connectomes, with distinct alterations in hub connectivity characterizing both modalities. More importantly, functional and anatomical modular connectomics interact to influence seizure burden. As hypothesized, the (extended) functional DMN broke down into separate anterior and posterior parts in TLE, corroborating previous studies.[4–6] We show that both the aDMN and pDMN lose internal communication, but that particularly the pDMN gains pathological long-range connectivity to other functional modules in TLE. This DD correlates with higher seizure frequency, but not duration.

In computational epilepsy models, changes in specific functional connection types and particularly hub-associated connectivity greatly impact seizure vulnerability.[17–19] Network segregation into more independent modules is thought to be a mechanism for containment of (pathological) activity, suggesting that increased functional connectivity between modules leads to higher seizure frequency.[43] In epileptic rodent medial temporal lobe, areas with high long-range hub connectivity are responsible for generation of seizures that spread throughout the entire hippocampus.[16,17] We have shown positive correlations between seizure frequency and functional between-module connectivity of the tumor in glioma patients.[24] Our results concerning the shift of within-module to between-module DMN hub connectivity and its correlation with seizure frequency in TLE corroborate these studies.

Why does this shift occur, and why is it specific to the DMN? In healthy brains, DMN areas form important functional hubs,[44,45] with efficient connectivity in the precuneus, posterior cingulate, and inferior parietal cortices associated with cognition and behavior.[46,47] Modeling brain activity onto anatomical networks shows that hubs are more vulnerable to functional dysfunction exactly because of their high use.[48] This may render the DMN the go-to spot for neurological diseases in general. For instance, Alzheimer's disease is accompanied by decreases in functional DMN hub functioning, with pathological amyloid deposition and atrophy spatially overlapping the DMN.[44] This apparent hub preference for dysfunctioning combined with high connectivity to all other subsystems may lead to global connectomic impairment when the DMN becomes implicated.[49,50] We term this hypothetical sequence of events a "catastrophic connectomic cascade".

Our study does not address the mechanism underlying this cascade of connectomic changes in TLE. Connectivity between the ipsilateral medial temporal lobe and the rest of the DMN may relate to either poorer[51] or better[52] memory functioning in TLE, depending on the study. Increased connectivity to and within the contralateral DMN has been linked to better cognitive performance as a "compensatory mechanism".[51–54] Speculatively, increased DMN connectivity relates to preserved cognitive functioning in TLE, although this increase is also accompanied by an increase in seizure frequency. Interestingly, increased within-module connectivity but decreased between-module connectivity, both functionally and anatomically, are linked to better cognitive functioning in children with frontal lobe epilepsy, although this study did not assess correlations with seizure vulnerability.[55] Previous studies in TLE only using regular connectivity instead of modular connectivity have indicated the importance of DMN integrity for cognitive functioning. Decreased communication between the aDMN and pDMN is linked to poorer episodic memory capacity and disturbed working memory,[4,52,56] suggesting that a link with cognitive functioning may well be present using modular connectivity as well.

Another possibility is that these increases in DMN connectivity are a pathological side effect of TLE, and that other mechanisms support continued cognitive functioning. In this framework, increased connectivity may reflect aberrant plasticity that impacts functioning negatively in the long run, as has been suggested in stroke.[57] Replicating our results in patients with cognitive testing would clarify these hypotheses.

The temporal development of this catastrophic connectomic cascade remains unknown. In TLE, negative correlations between temporal and lateral frontal lobe connectivity and disease duration have been reported,[58,59] but hub connectivity changes in the DMN have not been investigated. In our study, seizure frequency and disease duration were correlated, preventing us from separating their effects.

TLE patients also had increased functional within-module connectivity in the POM. The significance of these results remains unknown, as only one study in frontal lobe epilepsy also reports unexplained increased regular connectivity in the calcarine and lingual cortices.[60]

Anatomically, TLE patients displayed global losses of between-module connectivity. Previous studies have shown decreased white matter integrity,[7,61] with local increases in clustering and efficiency.[8,9] Global loss of between-module connectivity seems evident from earlier and current work.[8] Corroborating modeling studies,[43] this sign of increased modular segregation was associated with diminished seizure frequency, suggesting that an anatomically more compartmentalized connectome is favorable for seizure vulnerability. A problem with this interpretation is that patients with higher seizure frequency were more comparable to healthy controls in terms of between-module connectivity.

Again, the effect of time on the anatomical connectome may relate to these findings. The positive association between seizure frequency and anatomical between-module connectivity was not affected by seizure duration. However, seizure duration and frequency were correlated, which makes distinction between these two factors difficult. Almost certainly, anatomical connectomics in TLE are related to dynamics of the disease, albeit not on a linear time scale. Instead of viewing anatomical connectomics as an endpoint of gradual change, it could be at any of a range of intermediate states: patients may have decompensated first, after which compensatory change could have occurred. Future longitudinal investigations are necessary to further study these dynamics.

We replicated correlations between anatomical and functional connectomics in TLE,[5,14] but specified which types of multimodal hub connectivity are correlated while adding important insights about associations with seizure frequency. The association between DD and increased seizure frequency was mediated by higher anatomical between-module connectivity. However, higher seizure frequency also related to higher anatomical between-module connectivity through the mediating effects of modular DD. This indicates a vicious circle of seizures, disturbed DMN integrity and abnormal modular anatomical connectomics. The unpredictable, nonlinear transition from local anatomical damage to global connectomic dysfunction has also been shown in modeling work,[62] further underlining the necessity of viewing TLE as a highly

dynamical disease in which anatomy and function need to be taken into account as separate but interacting entities. Of course, these mediation analyses are statistical in nature, and our cross-sectional design does not allow for investigation of causality in any way.

Where do these results leave us in terms of clinical care? Interestingly, normalization of connectivity within the DMN after surgical intervention in TLE is positively correlated with memory outcome,[52] supporting the view that (restoration of) DMN integrity is pivotal in TLE. Combined with our results, hub connectivity signature may be a sensitive predictor of functioning in terms of both cognition and seizure burden. There may also be more direct methods of using connectomics to patients' benefit: perturbing the brain by means of magnetic or electric stimulation may alter DMN connectomics (among others), hereby improving functioning.[63] Indeed, several studies report improvement of symptoms in epilepsy patients after brain stimulation.[64] Future investigations are needed to assess the effects of stimulation on DMN hub connectivity.

Some study limitations should be kept in mind. First, there were some confounding differences between patients and controls (age, rsfMRI sequence, relative motion). We have taken every possible measure to minimize effects of age and motion on our results. The impact of sequence could not be mitigated, although its influence may be limited.[42] More importantly, the association between anatomical and functional hub connectomics and its clinical implications was determined within patients and is thus unaffected. Second, network analysis can be done in several ways. Using a proportional threshold diminishes the possibility of overall differences in connectivity between groups leading to network topology differences, supported by the robustness of our results when using more strict thresholds. Third, our modularity analyses placed both medial and lateral areas into the same module. Although these results are comparable to studies using the same modularity algorithm,[65] they differ slightly from others. Fourth, although some studies (generally with smaller sample size) report connectomic differences between RTLE and LTLE patients,[4,66] we only found significantly lower anatomical between-module connectivity in RTLE patients. Drug-refractory epilepsy TLE may only represent a subgroup of TLE, therefore potentially causing a selection bias in our study. Also, right and left TLE may be associated with different clinico-pathological features. In our study, RTLE patients had significantly lower seizure frequency, which prevents us from drawing definite conclusions regarding the influence of lateralization alone on connectomics. However, lateralization being a nonsignificant factor in almost all analyses suggests that the results described are common effects of TLE, regardless of affected hemisphere.

In conclusion, TLE is a multimodal connectomic disease, which impacts anatomical and functional hub connectivity differently. Shifts in functional hub connections from within to outside the DMN, an overall loss of integrative anatomical communication, and the interaction between these two increase seizure frequency.

Acknowledgments

This study was supported by NCRR (S10RR014978), National Institutes of Health (R01-NS069696, 5R01-NS060918, U01MH093765), and Dutch Organization for Scientific Research (NWO Rubicon 825.11.002). Our gratitude goes out to Cornelis J. Stam (department of Clinical Neurophysiology, VU University Medical Center, Amsterdam, the Netherlands) for fruitful discussions on the manuscript, and Dylan Tisdall and Andre van der Kouwe (both department of Radiology, Athinoula A. Martinos Center for Biomedical Imaging, Massachusetts General Hospital, Charlestown, MA, USA) for their help in developing MR sequences.

Conflict of Interest

Dr. Reinsberger reports grants from Epilepsy Foundation, during the conduct of the study; other from Sleep Med Inc., outside the submitted work. Dr. Douw reports grants from Dutch organization for research (NWO) Rubicon grant, during the conduct of the study.

References

1. Gusnard DA, Raichle ME. Searching for a baseline: functional imaging and the resting human brain. Nat Rev Neurosci 2015;2:338–352.
2. Van Diessen E, Diederen SJH, Braun KPJ, et al. Functional and structural brain networks in epilepsy: what have we learned? Epilepsia 2013;54:1855–1865.
3. Cataldi M, Avoli M, de Villers-Sidani E. Resting state networks in temporal lobe epilepsy. Epilepsia 2013;54:2048–2059.
4. Haneef Z, Lenartowicz A, Yeh HJ, et al. Effect of lateralized temporal lobe epilepsy on the default mode network. Epilepsy Behav 2012;25:350–357.
5. Liao W, Zhang Z, Pan Z, et al. Default mode network abnormalities in mesial temporal lobe epilepsy: a study combining fMRI and DTI. Hum Brain Mapp 2011;32:883–895.
6. Luo C, Qiu C, Guo Z, et al. Disrupted functional brain connectivity in partial epilepsy: a resting-state fMRI study. PLoS One 2011;7:e28196.

7. Vaessen MJ, Jansen JFA, Vlooswijk MCG, et al. White matter network abnormalities are associated with cognitive decline in chronic epilepsy. Cereb Cortex 2012;22:2139–2147.
8. DeSalvo M, Douw L, Tanaka N, et al. Altered structural connectome in temporal lobe epilepsy. Radiology 2014;270:842–848.
9. Bonilha L, Nesland T, Martz GU, et al. Medial temporal lobe epilepsy is associated with neuronal fibre loss and paradoxical increase in structural connectivity of limbic structures. J Neurol Neurosurg Psychiatry 2012;83:903–909.
10. Honey CJ, Kotter R, Breakspear M, Sporns O. Network structure of cerebral cortex shapes functional connectivity on multiple time scales. Proc Natl Acad Sci USA 2007;104:10240–10245.
11. Van den Heuvel MP, Mandl RC, Kahn RS, Hulshoff Pol HE. Functionally linked resting-state networks reflect the underlying structural connectivity architecture of the human brain. Hum Brain Mapp 2009;30:3127–3141.
12. Zhang Z, Liao W, Chen H, et al. Altered functional-structural coupling of large-scale brain networks in idiopathic generalized epilepsy. Brain 2011;134(Pt 10):2912–2928.
13. Voets NL, Beckmann CF, Cole DM, et al. Structural substrates for resting network disruption in temporal lobe epilepsy. Brain 2012;135(Pt 8):2350–2357.
14. Holmes MJ, Yang X, Landman BA, et al. Functional networks in temporal-lobe epilepsy: a voxel-wise study of resting-state functional connectivity and gray-matter concentration. Brain Connect 2013;3:22–30.
15. Czarnecki A, Tscherter A, Streit J. Network activity and spike discharge oscillations in cortical slice cultures from neonatal rat. Eur J Neurosci 2012;35:375–388.
16. Bonifazi P, Goldin M, Picardo MA, et al. GABAergic hub neurons orchestrate synchrony in developing hippocampal networks. Science 2009;326:1419–1424.
17. Morgan RJ, Soltesz I. Nonrandom connectivity of the epileptic dentate gyrus predicts a major role for neuronal hubs in seizures. Proc Natl Acad Sci USA 2008;105:6179–6184.
18. Dyhrfjeld-Johnsen J, Santhakumar V, Morgan RJ, et al. Topological determinants of epileptogenesis in large-scale structural and functional models of the dentate gyrus derived from experimental data. J Neurophysiol 2007;97:1566–1587.
19. Netoff TI, Clewley R, Arno S, et al. Epilepsy in small-world networks. J Neurosci 2004;24:8075–8083.
20. Newman ME. Analysis of weighted networks. Phys Rev E Stat Nonlin Soft Matter Phys 2004;70(5 Pt 2):56131.
21. Meunier D, Lambiotte R, Bullmore ET. Modular and hierarchically modular organization of brain networks. Front Neurosci 2011;4:200.
22. Moussa MN, Steen MR, Laurienti PJ, Hayasaka S. Consistency of network modules in resting-state FMRI connectome data. PLoS One 2012;7:e44428.
23. Guimera R, Nunes Amaral LA. Functional cartography of complex metabolic networks. Nature 2005;433:895–900.
24. Douw L, de Groot M, van Dellen E, et al. Local MEG networks: the missing link between protein expression and epilepsy in glioma patients? Neuroimage 2013;75:195–203.
25. Fischl B, van der Kouwe A, Destrieux C, et al. Automatically parcellating the human cerebral cortex. Cereb Cortex 2004;14:11–22.
26. Gerhard S, Daducci A, Lemkaddem A, et al. The connectome viewer toolkit: an open source framework to manage, analyze, and visualize connectomes. Front Neuroinform 2011;5:3.
27. Daducci A, Gerhard S, Griffa A, et al. The connectome mapper: an open-source processing pipeline to map connectomes with MRI. PLoS One 2012;7:e48121.
28. Desikan RS, Ségonne F, Fischl B, et al. An automated labeling system for subdividing the human cerebral cortex on MRI scans into gyral based regions of interest. Neuroimage 2006;31:968–980.
29. Smith SM, Jenkinson M, Woolrich MW, et al. Advances in functional and structural MR image analysis and implementation as FSL. Neuroimage 2004;23:S208–S219.
30. Yeo BTT, Krienen FM, Sepulcre J, et al. The organization of the human cerebral cortex estimated by intrinsic functional connectivity. J Neurophysiol 2011;106:1125–1165.
31. Conturo TE, Lori NF, Cull TS, et al. Tracking neuronal fiber pathways in the living human brain. Proc Natl Acad Sci USA 1999;96:10422–10427.
32. Cheng H, Wang Y, Sheng J, et al. Characteristics and variability of structural networks derived from diffusion tensor imaging. Neuroimage 2012;61:1153–1164.
33. Rubinov M, Sporns O. Complex network measures of brain connectivity: uses and interpretations. Neuroimage 2010;52:1059–1069.
34. Good BH, de Montjoye YA, Clauset A. Performance of modularity maximization in practical contexts. Phys Rev E Stat Nonlin Soft Matter Phys 2010;81(4 Pt 2):46106.
35. Benjamini Y, Hochberg Y. Controlling the false discovery rate: a practical and powerful approach to multiple testing. J R Stat Soc Series B 1995;57:289–300.
36. Preacher KJ, Hayes AF. Asymptotic and resampling strategies for assessing and comparing indirect effects in multiple mediator models. Behav Res Methods 2008;40:879–891.
37. Engel J. Surgical treatment of the epilepsies. New York, NY: Raven Press, 1987.

38. Fair DA, Cohen AL, Power JD, et al. Functional brain networks develop from a "local to distributed" organization. PLoS Comput Biol 2009;5:e1000381.
39. Dice LR. Measures of the amount of ecologic association between species. Ecology 1945;26:297–302.
40. Van Dijk KRA, Sabuncu MR, Buckner RL. The influence of head motion on intrinsic functional connectivity MRI. Neuroimage 2012;59:431–438.
41. Mowinckel AM, Espeseth T, Westlye LT. Network-specific effects of age and in-scanner subject motion: a resting-state fMRI study of 238 healthy adults. Neuroimage 2012;63:1364–1373.
42. Van Dijk KRA, Hedden T, Venkataraman A, et al. Intrinsic functional connectivity as a tool for human connectomics: theory, properties, and optimization. J Neurophysiol 2010;103:297–321.
43. Kaiser M, Hilgetag CC. Optimal hierarchical modular topologies for producing limited sustained activation of neural networks. Front Neuroinform 2010;4:8.
44. Buckner RL, Sepulcre J, Talukdar T, et al. Cortical hubs revealed by intrinsic functional connectivity: mapping, assessment of stability, and relation to Alzheimer's disease. J Neurosci 2009;29:1860–1873.
45. Achard S, Salvador R, Whitcher B, et al. A resilient, low-frequency, small-world human brain functional network with highly connected association cortical hubs. J Neurosci 2006;26:63–72.
46. Van den Heuvel MP, Stam CJ, Kahn RS, Hulshoff Pol HE. Efficiency of functional brain networks and intellectual performance. J Neurosci 2009;29:7619–7624.
47. Sestieri C, Corbetta M, Romani G, Shulman GL. Episodic memory retrieval, parietal cortex, and the default mode network: functional and topographic analyses. J Neurosci 2011;31:4407–4420.
48. De Haan W, Mott K, van Straaten ECW, et al. Activity dependent degeneration explains hub vulnerability in Alzheimer's disease. PLoS Comput Biol 2012;8:e1002582.
49. Honey CJ, Sporns O. Dynamical consequences of lesions in cortical networks. Hum Brain Mapp 2008;29:802–809.
50. Alstott J, Breakspear M, Hagmann P, et al. Modeling the impact of lesions in the human brain. PLoS Comput Biol 2009;5:e1000408.
51. Holmes M, Folley BS, Sonmezturk HH, et al. Resting state functional connectivity of the hippocampus associated with neurocognitive function in left temporal lobe epilepsy. Hum Brain Mapp 2014;35:735–744.
52. McCormick C, Quraan M, Cohn M, et al. Default mode network connectivity indicates episodic memory capacity in mesial temporal lobe epilepsy. Epilepsia 2013;54:809–818.
53. Bettus G, Wendling F, Guye M, et al. Enhanced EEG functional connectivity in mesial temporal lobe epilepsy. Epilepsy Res 2008;81:58–68.
54. Bettus G, Guedj E, Joyeux F, et al. Decreased basal fMRI functional connectivity in epileptogenic networks and contralateral compensatory mechanisms. Hum Brain Mapp 2009;30:1580–1591.
55. Vaessen MJ, Jansen JFA, Braakman HMH, et al. Functional and structural network impairment in childhood frontal lobe epilepsy. PLoS One 2014;9:e90068.
56. McCormick C, Protzner AB, Barnett AJ, et al. Linking DMN connectivity to episodic memory capacity: what can we learn from patients with medial temporal lobe damage? Neuroimage Clin 2014;5:188–196.
57. Carter AR, Shulman GL, Corbetta M. Why use a connectivity-based approach to study stroke and recovery of function? Neuroimage 2012;62:2271–2280.
58. Zhang Z, Lu G, Zhong Y, et al. Altered spontaneous neuronal activity of the default-mode network in mesial temporal lobe epilepsy. Brain Res 2010;1323:152–160.
59. Liao W, Zhang Z, Pan Z, et al. Altered functional connectivity and small-world in mesial temporal lobe epilepsy. PLoS One 2010;5:e8525.
60. Widjaja E, Zamyadi M, Raybaud C, et al. Abnormal functional network connectivity among resting-state networks in children with frontal lobe epilepsy. AJNR Am J Neuroradiol 2013;34:2386–2392.
61. Liacu D, Idy-Peretti I, Ducreux D, et al. Diffusion tensor imaging tractography parameters of limbic system bundles in temporal lobe epilepsy patients. J Magn Reson Imaging 2012;36:561–568.
62. Van Dellen E, Hillebrand A, Douw L, et al. Local polymorphic delta activity in cortical lesions causes global decreases in functional connectivity. Neuroimage 2013;83:524–532.
63. Liston C, Chen AC, Zebley BD, et al. Default mode network mechanisms of transcranial magnetic stimulation in depression. Biol Psychiatry 2014;76:517–526.
64. Kimiskidis VK, Valentin A, Kälviäinen R. Transcranial magnetic stimulation for the diagnosis and treatment of epilepsy. Curr Opin Neurol 2014;27:236–241.
65. Meunier D, Achard S, Morcom A, Bullmore E. Age-related changes in modular organization of human brain functional networks. Neuroimage 2009;44:715–723.
66. Morgan VL, Sonmezturk HH, Gore JC, Abou-Khalil B. Lateralization of temporal lobe epilepsy using resting functional magnetic resonance imaging connectivity of hippocampal networks. Epilepsia 2012;53:1628–1635.

